



Article

Accuracy Assessment of Total Stem Volume Using Close-Range Sensing: Advances in Precision Forestry

Dimitrios Panagiotidis *  and Azadeh Abdollahnejad 

Faculty of Forestry and Wood Sciences, Czech University of Life Sciences (CZU Prague), Kamýčká 129, 165 21 Prague, Czech Republic; abdollahnejad@fld.czu.cz

* Correspondence: panagiotidis@fld.czu.cz; Tel.: +420-775-099-596

Abstract: Accurate collection of dendrometric information is essential for improving decision confidence and supporting potential advances in forest management planning (FMP). Total stem volume is an important forest inventory parameter that requires high accuracy. Terrestrial laser scanning (TLS) has emerged as one of the most promising tools for automatically measuring total stem height and diameter at breast height (DBH) with very high detail. This study compares the accuracy of different methods for extracting the total stem height and DBH to estimate total stem volume from TLS data. Our results show that estimates of stem volume using the random sample consensus (RANSAC) and convex hull and H_{TSP} methods are more accurate (bias = 0.004 for RANSAC and bias = 0.009 for convex hull and H_{TSP}) than those using the circle fitting method (bias = 0.046). Furthermore, the RANSAC method had the best performance with the lowest bias and the highest percentage of accuracy (78.89%). The results of this study provide insight into the performance and accuracy of the tested methods for tree-level stem volume estimation, and allow for the further development of improved methods for point-cloud-based data collection with the goal of supporting potential advances in precision forestry.



Citation: Panagiotidis, D.; Abdollahnejad, A. Accuracy Assessment of Total Stem Volume Using Close-Range Sensing: Advances in Precision Forestry. *Forests* **2021**, *12*, 717. <https://doi.org/10.3390/f12060717>

Academic Editor: John Couture

Received: 5 May 2021
Accepted: 29 May 2021
Published: 31 May 2021

Publisher's Note: MDPI stays neutral with regard to jurisdictional claims in published maps and institutional affiliations.



Copyright: © 2021 by the authors. Licensee MDPI, Basel, Switzerland. This article is an open access article distributed under the terms and conditions of the Creative Commons Attribution (CC BY) license (<https://creativecommons.org/licenses/by/4.0/>).

Keywords: dendrometry; terrestrial laser scanner; ArcGIS; RANSAC; circle fitting; convex hull; tree stem modelling; tree-level assessment

1. Introduction

In most countries, forest inventories are based on statistical sampling with traditional field measurements, which are usually costly, time-consuming, and laborious. However, the increasing demand for resources for human welfare, environmental protection, and conservation requires even higher precision and faster processing of forest inventories. Stem volume is an important input for basic forest inventories that helps in economic forecasting, decision making, and sustainable timber resource planning [1,2]. Moreover, stem volume cannot be measured directly, but must be modeled and predicted from other variables that are more easily measured. Stem volume is a function of the two main tree variables: (a) diameter at breast height (DBH), and (b) tree height [3,4]. Diameter is measured using either calipers or a logging tape [5], while tree height is commonly measured using clinometer, laser rangefinder, or hypsometer based on ultrasonic technology [6,7].

Unbiased measurements of stem volume at the tree level are important because they can provide information that can help in estimating the effects of forestry activities on carbon stocks and, thus, on climate regulation [8,9]. The accuracy of stem measurements using traditional methods has recently been questioned in several studies. Apart from the fact that traditional methods are a very tedious process, there is also a high uncertainty in the way field measurements are made.

Today, stem variables can be measured with high accuracy using terrestrial laser scanning (TLS) devices. Several studies have been conducted to derive tree height [3,7,10,11], DBH [7,10], and plot basal area [12,13] from point clouds. Tree detection and stem dimension estimation with TLS are common methods for tree-level stem volume prediction [7,14].

Point cloud processing for DBH extraction can be performed using various mathematical models defined by a circle or an ellipse. These models can be divided into two main categories: algebraic, and geometric. Some of the most common algebraic methods based on least square fitting are those of Pratt [15], Kasa [16], Taubin [17], Chernov [18], and Fitzgibbon [19]. On the other hand, the most common geometric methods include random sample consensus (RANSAC) [20,21], Hough transform [22,23], skeletonization [24], and convex hull [25].

Olofsson et al. [22] used a modified version of RANSAC and the Hough transform to develop and validate a new method for detecting, classifying, and measuring tree stems and canopies. Their results showed that the most accurate diameter measurements for pines were obtained with an RMSE of 7% for a defined plot radius of 20 m. In 2016, Mikita et al. [25] compared two automatic methods for processing point clouds and delineating the stem circumference at breast height. Their results showed that the RMSE for DBH estimation ranged from 0.9 cm to 1.8 cm for the two circumscribed circle and convex hull methods tested, respectively.

The most common methods for estimating tree height from point clouds are based on digital elevation models (DEMs). In a recent study, Wang et al. [3] generated digital terrain models (DTMs) from multi-scan TLS and aerial laser scanning (ALS) data to estimate total stem height. Their results showed that the data from ALS had better performance for taller trees, while TLS had better performance for trees up to 20 m. In another work, Panagiotidis et al. [11] used different height extraction methods for estimating tree height based on canopy height models (CHMs) and local maxima. Their method proved to be reliable for height estimation of trees up to 30 m, for both deciduous and coniferous trees.

There are several studies on estimation of stem volume using TLS. Astrup et al. [26] evaluated volume estimates derived from standard volume functions and TLS data compared to traditional measurements. They found that tree volume could be estimated from TLS with high precision and accuracy; Spearman's correlation coefficients ranged from 0.77 to 0.97. In 2021, Panagiotidis et al. [7] compared the difference between total stem volume from TLS and traditional inventory data. The coefficient of determination showed a strong relationship between measured and estimated stem volume, with an $R^2 = 0.87$ for deciduous trees and $R^2 = 0.98$ for conifers. In a former study, Mayamanikandan et al. [27] investigated the performance of DBH and tree height in evaluating stem volume. Their results showed that there was good agreement with the reference data for height ($R^2 = 0.99$), DBH ($R^2 = 0.99$), and stem volume ($R^2 = 0.96$).

This work contributes to characterizing the accuracy of stem volume estimates derived from TLS data compared to traditional forest inventory data, by testing different automated methodological approaches to total stem height and DBH. This will provide insight into the tree-level performance and accuracy of these methods, with the goal of supporting potential advances in precision forestry.

2. Materials and Methods

2.1. Characterization of the Test Site

The experiment was conducted in the School of Forest Enterprise of the Czech University of Life Sciences (ČZU Prague) in Kostelec and Černými Lesy (Figure 1). The study area extends geographically from 49°54'50.19" N; 14°52'23.61" E to 49°54'50.12" N; 14°52'24.98" E., with an area of 25 m² (25 × 25 m). In terms of species composition, the area is dominated by Norway spruce (*Picea abies* (L.) H. Karst.). The expanded area is mainly characterized by managed, even-aged forests with an age of about 60 years. In addition, artificial branch pruning has been carried out in the past for the lower portions of trees. The terrain profile in the area is gently sloping, with an elevation of about 420 m ASL, a mean annual temperature of 7.5 °C, and a mean annual precipitation of 600 mm.

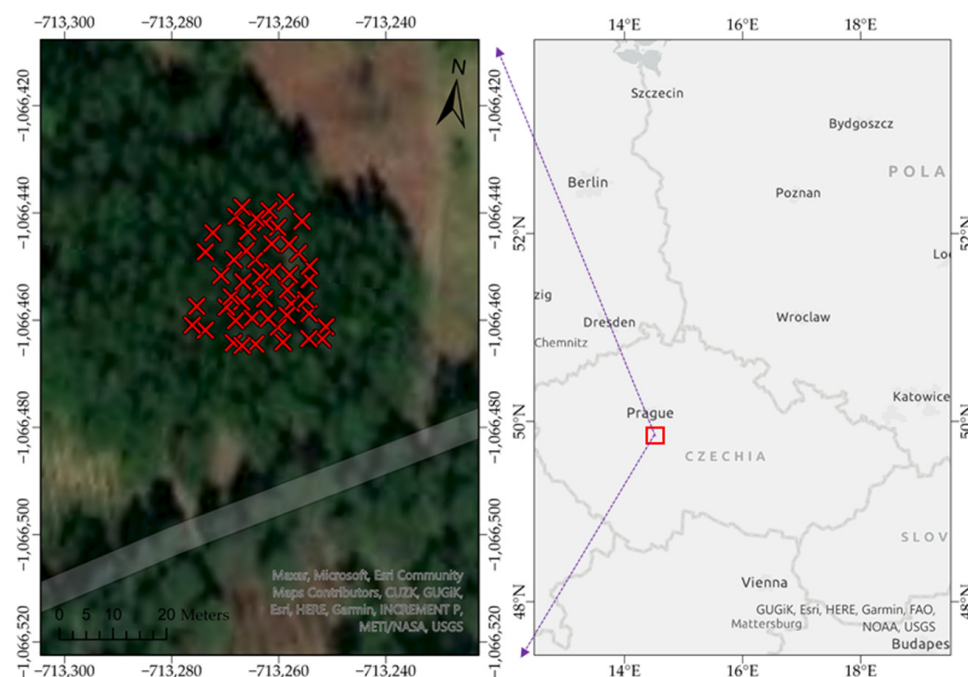


Figure 1. Map of Czechia with the geographic location of the study area.

2.2. Reference Data Acquisition

A Trimble M3 total station (Trimble Inc. Sunnyvale, CA, USA, 1978) was used to survey the tree locations using the independent coordinate system, and helped to verify the exact locations (at 100 m, the error range is ± 23 mm) of trees from TLS. The total height of the trees was determined using a Haglöf Laser Geo (distance accuracy 40 mm) [28]; to avoid biased estimates, the distance from each tree was at least equivalent to the tree's height. DBH was determined with millimeter accuracy using a Haglöf DP II (Haglöf Sweden AB, Långsele, Sweden, 2002) computer caliper [29]. Preliminarily, all stems were marked with a spray at DBH to increase the consistency of the measurements. For each tree, two diameters were manually measured from perpendicular directions, and DBH was then determined as the average of these two measurements. In total, we measured 48 trees.

2.3. TLS Measurements

The Trimble TX8 scanning system (Trimble Inc., Sunnyvale, CA, USA, 1978) was used for this study, and the technical specifications of the TLS device are given in Table 1. To ensure the optical degree of overlapping between the scanning positions we used the multi-scan approach, with a total of seven scans. The first scan was placed in the center of each plot, and the rest in its periphery. In addition to the scan parameters, fixed exposure was disabled, while third level mode was used for the scan density. The device provides $360^\circ \times 317^\circ$ field-of-view acquisition, enabling optimal scanning performance of high-resolution scans up to 120 m, and generating 555 Mpts (million points) per scan in third level mode. The duration for each scan was 10 min. The field instant method was used to calibrate the laser scanner. Furthermore, to ensure better performance in the scan registration, the laser scanner reference sphere set of the laser scanner was used [30]. Marked wooden sticks were placed on the ground at each station in parallel with the scans; this allowed the scan positions to be measured with the Trimble M3 total station, with an error of 2 mm in horizontal distance. The registration of the point cloud was conducted using RealWorks software (Trimble Inc., Sunnyvale, CA, USA, 1978), with a point density of 0.01 m. Laser scanning was performed on 26 August 2019.

Table 1. Trimble TX8 terrestrial laser scanning device specifications.

Range Measurement	
Maximum Distance Range	120 m on most surfaces
Range Systematic Error	<2 mm
Laser Wavelength	1.5 μm , invisible
Laser Beam Diameter	6–10–34 mm @ 10–30–100 m
Scanning Field-of-View	360° \times 317°
Scanning Speed	1 million pts/s
Angular Accuracy	80 μrad

2.4. Point Cloud Normalization

Firstly, we computed the distances between ground and off-ground points, in order to eliminate the differences in total stem height caused by differences in elevation using the cloth simulation filter (CSF) algorithm [31] in CloudCompare (V.2.11.3 Zephyrus, Paris, France, 2011) [32]. Thus, tree locations were transformed to a horizontal plane with the same elevation. Ground and off-ground points were then extracted as LAS files and imported into ArcGIS Pro V2.7.2 (ESRI Inc., Redlands, CA, USA) [33] to create the DTM and digital surface model (DSM), with an accuracy of 0.01×0.01 m cell size.

2.4.1. Total Stem Height Estimation from H_{TSP} and Tree Locations

For the estimation of total stem height, we relied on the results of our previous work, in which we analyzed the differences in modelling total stem height, using two different height estimation methods for the same data. The results showed that the method of the centers of stem cross-sections at stump height (~30 cm off the ground) [34] (H_{TSP}) performed better than treetop detection based on local maxima (H_{TTD}) [7]. A kernel window size of 2 m was used; the decision for the optimal kernel window size was straightforward since the application of local maxima on coniferous trees can successfully detect a single treetop per tree [11]. As a result of the above analysis, and based on the hypothesis that all trees in the study area had a cylindrical stem shape, we used a hypothetical vertical axis parallel to the z-axis in order to connect the treetop with the center of each stem cross-section at stump height (H_{TSP}), considering only the nearest values around that vertical axis. By overlaying the generated normalized canopy height model (nCHM) [35] and tree stump locations based on the center of each stump cross-section, we were able to estimate the exact stem locations and extract the total stem height using the “feature to point” tool in ArcGIS Pro V2.7.2 [36] (Figure 2). The spatial resolution of the nCHM was 0.01×0.01 m cell size.

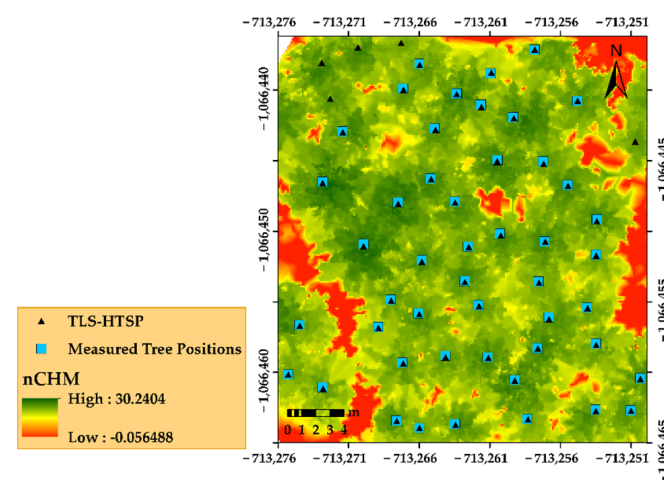


Figure 2. Normalized canopy height model (nCHM) and the stem locations. Unprocessed trees in the upper-left and -right corners are not part of this study.

2.4.2. Total Stem Height Estimation Using the RANSAC Method

We used the RANSAC method [22] in CloudCompare for point cloud shape determination of stems, as shown in Figure 3. In the general parameter settings tab of RANSAC shape detection, we used cylinder as the primitive and set 500 as the minimum number of support points per cylinder. In the advanced parameter settings, based on the size of each stem, we used maximum distance to the cylinder (e = default values), sampling resolution (b = default values), maximum normal deviation (a = default), and overlook probability (default). Once the algorithm iterated through all the stems, the total length (above the ground to the treetop) was extracted for each colored cylinder.

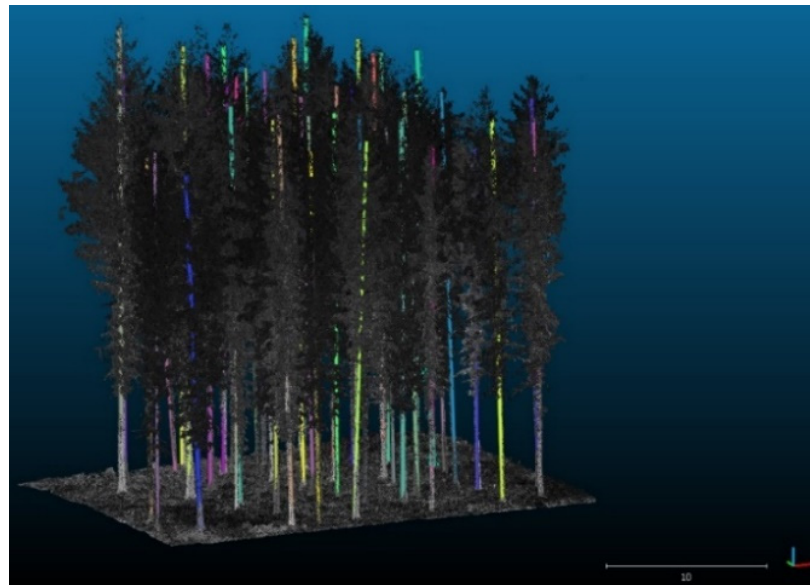


Figure 3. Scalar field color view of the study area, stem segmentation, and cylinder fitting using the random sample consensus (RANSAC) method.

2.5. Diameter Estimation

2.5.1. Geometric Approach by RANSAC

Similar to height estimation, we used the same parameters to apply the cylindrical fitting to estimate the DBH. In addition, we were able to use the “point picking” tool to measure and select all points between 1.25 and 1.35 m height above the ground, and then, by enabling the cylinder layer, the “cross section” tool was applied to extract all cylinder slices at that height (Figure 4c).

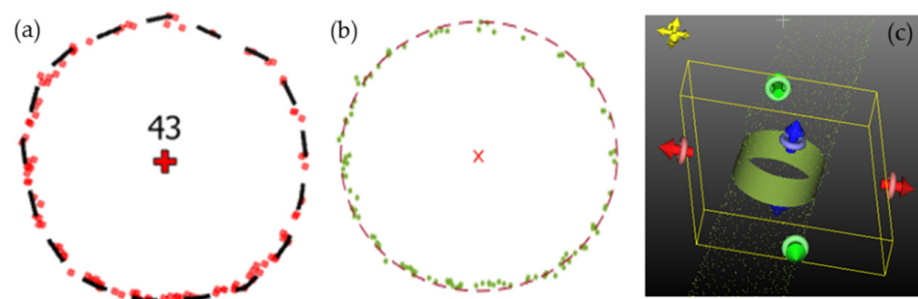


Figure 4. An example of the same cross-sectional profile and the different fitting methods at diameter at breast height (DBH) using (a) convex hull (the red points represent the TLS data, and the dashed black line represents the convex hull circumference), (b) circle fitting (green points represent the TLS data; the dashed red line represents the circle fitting circumference), and (c) RANSAC.

2.5.2. Algebraic Approach by Circle Fitting

The normalized points were used as inputs for estimating DBH in MATLAB R201b professional (MathWorks©, Inc., Natick, MA, USA), using the statistics and machine learning toolbox™. A buffer zone was applied to select all points between 1.25 and 1.35 m, using .Net framework in Visual Studio Enterprise 2015 V.14.0.24720.00 (Microsoft©, Redmond, Washington, DC, USA, 1975). The average number of selected points used to estimate the stem diameter for each stem was approximately 86. The points were then extracted as TXT files for further processing. We then estimated the stem radius in the produced stem cross-sections using the hierarchical cluster analysis (HCA) method [37]. This method allowed the formation of multiple clusters based on the total number of stems. First, we calculated the Euclidean distances between the (x, y) points using the function “pdist” (Equation (1)) as follows:

$$d(x, y) = \sqrt{(x_1 - y_1)^2 + (x_2 - y_2)^2} \quad (1)$$

where (x, y) are two points with coordinates $x = (x_1, x_2)$ and $y = (y_1, y_2)$.

Once the proximity between the points was calculated, we were able to determine how the stem cross-section points should be grouped into clusters using the “linkage” function. Ward’s minimum variance method in the “linkage” function was used to obtain the calculated distances and link pairs of (x, y) points into binary clusters, as seen in Equation (2):

$$d(r, s) = \sqrt{\frac{2n_r n_s}{(n_r + n_s)}} \times \|\bar{x}_r - \bar{x}_s\|_2 \quad (2)$$

where $\|\cdot\|_2$ is the Euclidean distance, \bar{x}_r and \bar{x}_s are the centroids of clusters (r) and (s) , respectively, and n_r and n_s refer to the number of elements in clusters (r) and (s) , respectively.

The “cluster” function was then used to specify arbitrary clusters to partition data into the desired number of clusters, based on the total number of stems. We used the method proposed by Bucher [38]. This method is a modified version of the [16] circle fitting method (Equation (3)), based on the least squares. The “circfit” function was used to fit a circle to a set of measured points:

$$[xc, yc, R, \sim] = \text{circfit}(x, y) \quad (3)$$

where xc, yc are the returned centers for each stem cross-section, R is the returned estimated radius, and parameters, a, b , and c , are optional coefficients describing the general circle form equation (Equation (4)):

$$x^2 + y^2 + a \times x + b \times y + c = 0 \quad (4)$$

As a final step, the constructed “circfit” function was iterated to ensure that all stem cross-section points were fitted, their respective radii were estimated, and would successfully be stored in cell arrays (Figure 4b).

2.5.3. Geometric Approach by Convex Hull

The cross-sectional areas at DBH used for the circle fitting method were also used to estimate DBH by the convex hull method. Initially, we converted the table to excel using the “excel to table” tool in ArcGIS Pro V2.7.2. In the generated table we assigned a unique code ID to each stem. The cross-sections were converted into geodatabase features using the local coordinate system S-JTSK/Krovak East North. Furthermore, the “minimum bounding geometry” tool was used to delineate polygons for each point cluster in order to approximate the shape of stem cross-sections. By using the “feature to point” tool, we were able to define the center of gravity (centroid) in each polygon; the horizontal centers of the stems were then exported as a new point layer. Finally, the “point distance” tool was used to calculate the distances between the center and the polygon vertices, using a

defined radius of 50 cm based on the size of our stems. The average radius was then used to define the stem diameter (Figure 4a).

Additionally, in the attribute table of the convex hull layer, an additional field was created for the characterization of stem cross-sections based on circularity. Circularity is a roundness error definition (Equation (5)) to identify which stem cross-sectional areas (produced by the convex hull) are closer to a perfect circular shape ($\overset{\text{Circularity}}{\rightarrow} 1^-$), and which deviate from a circular shape ($\overset{\text{Circularity}}{\rightarrow} 0^+$):

$$\text{Circularity}_{\text{stem cross-section}} = \frac{(4 * \pi * \text{area})}{\text{perimeter}^2} \quad (5)$$

2.6. Derivation of Total Stem Volume

Total stem volume was calculated using DBH as a predictor from observed and estimated (RANSAC, circle fitting, convex hull) values. As for the total stem height, the H_{TSP} method was used in the case of circle fitting and convex hull. For the estimation of total stem volume, the allometric equation for Norway spruce by Petráš and Pajčík [39] was applied (Equation (6), Table 2). In terms of suitability, Equation (6) is based on empirical data, calculated primarily for the standards of central Europe [39]:

$$V_{\text{Norway spruce}} = \left(A * (\text{DBH}_{1.3} + 1)^B * H^C \right) - \left(E * (\text{DBH}_{1.3} + 1)^F * H^G \right) \quad (6)$$

Table 2. The parameters used in Equation (6).

Norway Spruce	A	B	C	E	F	G
Coefficients	4.01×10^{-5}	1.821816	1.132062	9.29×10^{-3}	-1.02037	0.896101

2.7. Accuracy Assessment

First, we tested the normality of our data, and found out that the data were not normally distributed. Therefore, we used the Friedman analysis of variance (ANOVA), which is a non-parametric statistical test, while for the post-hoc analysis we used the Wilcoxon test for two related samples (i.e., observed vs. convex hull). For calculating the alpha for the post-hoc analysis, we used the Bonferroni correction (Equation (7)):

$$a' = \frac{a}{k} \quad (7)$$

The relationship between observed and estimated volume was modelled using linear regression. Accuracy assessment was performed at the tree level to evaluate the accuracy of the total stem volume obtained from the TLS by calculating the R-squared (Equation (8)):

$$R^2 = 1 - \frac{\sum_{i=1}^n (E_i - O_i)^2}{\sum_{i=1}^n (E_i - O_{\text{imean}})^2} \quad (8)$$

where E_i and O_i represent the estimated and observed values, O_{imean} refers to the average of the observed values, and n is the number of stems.

Additionally, box and whisker plots were used to illustrate the variance for the observed and estimated volume. Finally, we calculated *bias* (Equation (9)), and *bias%* (Equation (10)), as follows:

$$\text{Bias} = \frac{1}{n} \sum x_i - \bar{x}_j \quad (9)$$

$$\text{Bias}\% = \frac{\text{Bias}}{\bar{x}_j} \times 100 \quad (10)$$

From Equations (9) and (10), x_i is the observed value, \bar{x}_j is the average of estimated values, and n is the number of stems.

3. Results and Discussion

Firstly, we examined the correlation between the observed and estimated stem volume (Figure 5). Based on the R-squared results, circle fitting with $R^2 = 0.97$ had the highest correlation with the observed stem volume (Figure 5b). RANSAC with $R^2 = 0.68$ showed lower correlation with observed stem volume compared to circle fitting (Figure 5a). Finally, convex hull with $R^2 = 0.18$ had the lowest correlation with observed stem volume (Figure 5c). Therefore, we calculated the deviation of each DBH polygon generated from the convex hull and the actual circle shape, in order to examine the relationship between circularity and stem volume residuals (Figures 5c and 6). As the results suggested, there was no correlation between these two with $R^2 = 0.02$ (Figure 7).

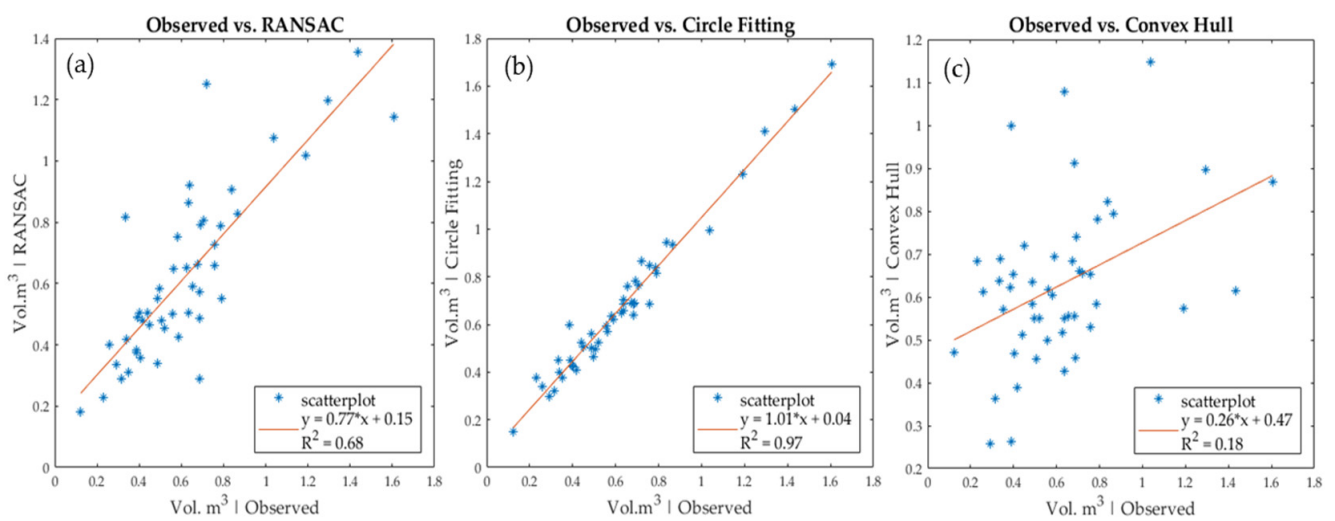


Figure 5. Linear regression models of the observed and estimated total stem volume between the three used approaches. (a) shows the volume correlation between observed and RANSAC, (b) shows the volume correlation between observed and circle fitting, and (c) shows the volume correlation between observed and convex hull.

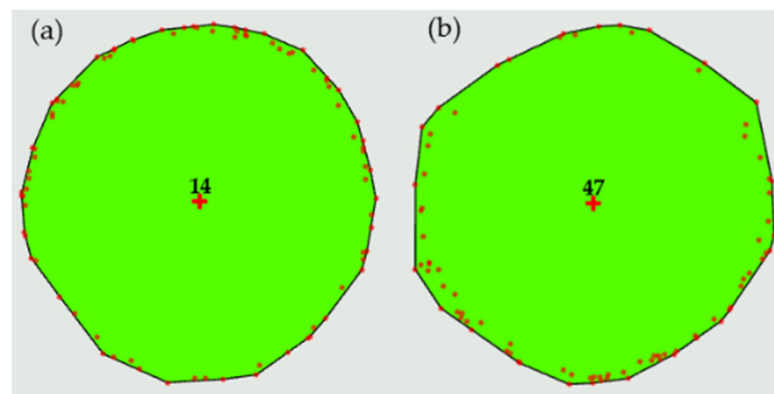


Figure 6. The deviation of stem shape profile from the regular circular shape, for a circularity of (a) 0.986, and (b) 0.974. The red points represent the TLS data, and the continuous black line represents the convex hull circumference. The numbers in the center represent the stem code ID.

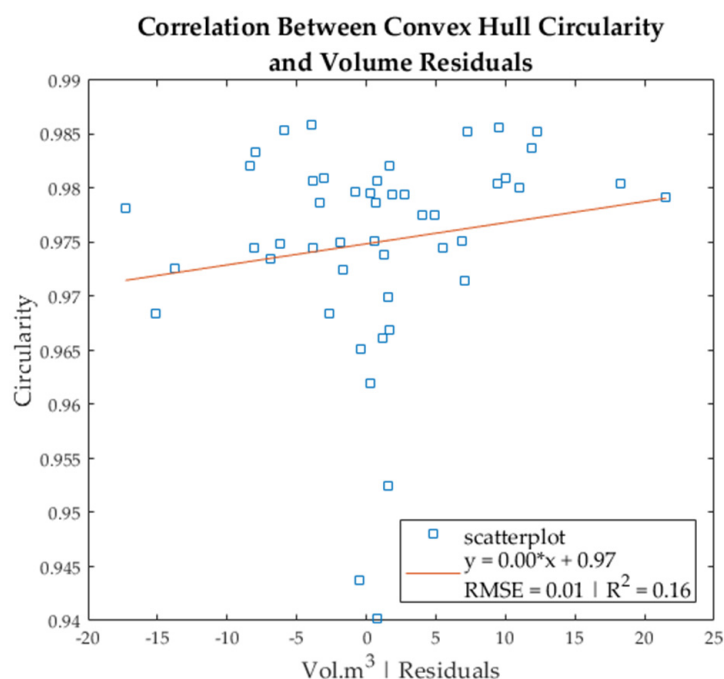


Figure 7. Correlation between the circularity (deviation of stem shape profile from regular circle) and the produced volume residuals (observed vs. convex hull).

Although no correlation was found between the convex hull circularity and stem volume residuals, this method can be used as a robust and automatic benchmark technique to identify any 2D shape that deviates from a regular circular shape. For example, objects with circularity less than 0.886 are considered to be squares. Since natural stem shapes are either circular, semi-circular (irregular), or elliptical, circularity can then be used to identify all the non-circular shapes over a large number of cross-sectional points.

The Friedman test exhibited significant differences between the different datasets (observed and estimated), with $\alpha = 0.05$ (Table 3), meaning that all or some of the estimated methods produced results that were significantly far from the observed values. To determine where these differences occurred, the Wilcoxon test was used. To reject the null hypothesis (H_0), the asymptotic significance (two-tailed) should be less than $\alpha = 0.0125$. This alpha value was calculated using the Bonferroni correction (Table 4), which is the division of the alpha value (0.05) by the total number of variables.

Table 3. Friedman test ($\alpha = 0.05$).

N *	48
Chi-Square	12.925
Df *	3
Asymptotic Significance	0.004801637

* N: number of observations; Df: degrees of freedom.

Table 4. Asymptotic significance based on post-hoc analysis (Wilcoxon test).

	Observed	Circle Fitting *	RANSAC	Convex Hull *
Observed	-	0.00	0.94	0.57
Circle Fitting *	0.00	-	0.06	0.63
RANSAC	0.94	0.06	-	0.70
Convex Hull *	0.57	0.63	0.70	-

* ($\alpha = 0.0125$) based on Bonferroni correction. Circle fitting and H_{TSP} ; convex hull and H_{TSP} .

According to the Wilcoxon test results, the estimated stem volume derived from circle fitting and H_{TSP} had a significant difference from the observed volume with $p = 0.00$.

However, there was no significant difference between circle fitting and the rest of the estimated results (Figure 8, Table 4). Moreover, the Wilcoxon test showed that, in most cases (42 out of 48), circle fitting resulted in an overestimation of values, leading to a higher amount of bias% (6.976%) (Table 5). Furthermore, the Wilcoxon test demonstrated that there was no significant difference between the estimated stem volume from convex hull ($p = 0.57$), RANSAC ($p = 0.94$) and the observed values (Table 4). Furthermore, compared to circle fitting, which overestimated stem volume 87.5% of the time, convex hull and RANSAC had almost equal amounts (~50%) of overestimation and underestimation of stem volume, resulting in lower amounts of bias%, at 1.456% and 0.672%, respectively (Table 5).

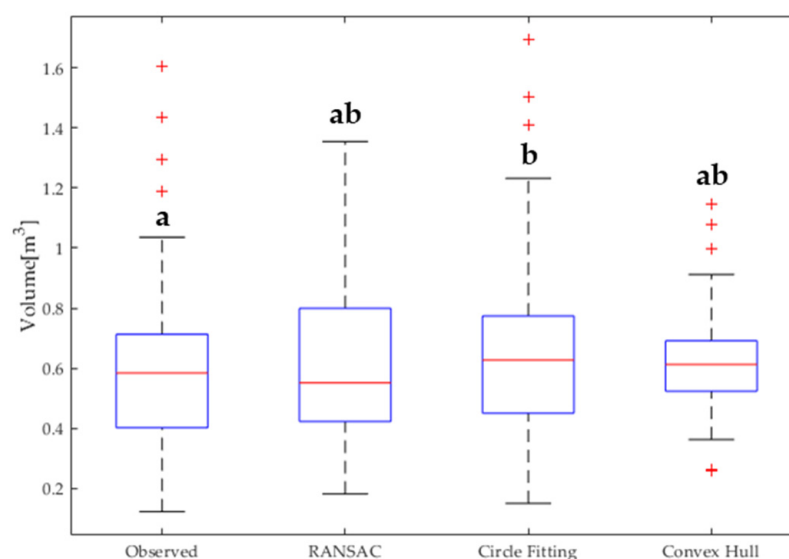


Figure 8. Box and whisker plots of the observed and estimated total stem volume. The letters (a and b) indicate whether or not there were significant differences between the groups at a 0.05 significance level.

Table 5. Wilcoxon signed-rank test.

Method	Negative Rank (Observed > Estimated)	Positive Rank (Observed < Estimated)	Ties
RANSAC	25	23	0
Circle Fitting and H_{TSP}	6	42	0
Convex Hull and H_{TSP}	23	25	0

Convex hull presented lower bias (0.01) and bias% (1.46) compared to circle fitting, with bias of 0.05 and bias% of 6.98. The results of convex hull are in accordance with the results of previous studies [25]. RANSAC, with bias 0.00 and bias% = 0.67, had the highest performance for the stem volume estimation (Figure 8, Table 6).

According to our results, RANSAC had better performance than the other two methods for the stem volume estimation, with low bias and no significant differences in determining the estimated stem volumes from the actual observed values. Moreover, RANSAC provides some desirable features, such as noise reduction, which is useful in dendrometry for extracting stem attributes, especially for complex forest structures. This method is robust, and can work with data containing a large number of outliers (more than 50%) [21,22].

Table 6. Statistical summary of the observed and estimated total stem volume.

	Observed Volume	Estimated Volume		
		RANSAC	Circle Fitting *	Convex Hull *
Mean	0.619	0.623	0.665	0.628
Min	0.123	0.182	0.151	0.258
Q1	0.403	0.424	0.451	0.527
Median	0.584	0.551	0.627	0.613
Q3	0.710	0.796	0.769	0.690
Max	1.606	1.354	1.694	1.147
Bias	0.000	0.004	0.046	0.009
Bias%	0.000	0.672	6.976	1.456

* Circle fitting and H_{TSP} ; convex hull and H_{TSP} .

In contrast, circle fitting had the lowest performance in estimating stem volume, with the largest bias. It also produced significantly different results compared to observed values due to the nature of the circle fitting method for determining the stem radius. As mentioned earlier, stems are usually not fully circular, in most cases being either semi-circular or elliptical. Moreover, the shapes of older or damaged trees are not well approximated by a circle, since they differ significantly from circular stem shapes. Therefore, in our case, RANSAC and convex hull, approximated all the stem shapes based on elliptical or irregular polygons, resulting in better performance for the stem volume estimation compared to circle fitting.

Additionally, it is evident that, in some cases, TLS position or tree location (i.e., border trees) may create inadequate data, leading to overestimation of stem attributes [40]. Apart from the nature of the circle fitting method, which slightly overestimated total stem volume, different TLS locations for the scale of our study area (25×25 m) would not have provided better results for circle fitting. Furthermore, the used TLS multi-scan approach produced a sufficient number of points along the stem circumference for all trees. Saarinen et al. [41] found similar results in a study on Norway spruce. The objective of the study was to investigate the effect of TLS data collection at different distances (i.e., 25%, 59%, 75%, and 100% of tree height). The results showed that longer distances increased the uncertainty when the scanning distance was greater than approximately 50% of the tree height, because the number of successfully measured diameters from the TLS point cloud was not sufficient for estimating stem volume. Similarly, a recent study [42] suggests that TLS point clouds can be used to predict stem volumes of individual trees, but the accuracy of the results depends mainly on the coverage of the original point cloud data and the used method.

Examination of trends in other studies that have used different modelling approaches, data types, sample sizes, etc., to estimate key forest variables has shown that proper selection of methods and statistics is critical to achieving accurate predictive models [43,44].

4. Conclusions

The use of TLS in modern forestry is a technology with high potential, which allows reliable and accurate reconstruction of stem geometry as long as the surface is sufficiently covered by points. In this paper we presented a benchmark assessment to investigate the accuracy of total stem volume at tree level from close-range sensing data, using different methodological approaches. Based on our results, the use of geometric approaches such as RANSAC and convex hull is recommended due to their ability to model irregular stem shapes with very low bias, thus improving the accuracy of stem attribute estimates. In contrast, the algebraic method presented in this paper considered the stem as a complete circle, causing biased estimates of stem diameter. According to the Wilcoxon test, the estimated volume derived from circle fitting and H_{TSP} showed a significant difference from the observed volume with $p = 0.00$. In other words, the relationship found between circle fitting and the observed data ($R^2 = 0.97$) was purely random, which means that repeating this method in a different sample set would not guarantee the same accuracy and performance. In our case, circle fitting resulted in an overestimation of stem volume

87.5% of the time. However, the other two methods (RANSAC and convex hull) provided accurate volume estimates with very low bias (0.004 for RANSAC and 0.009 for convex hull). The RANSAC method had the best performance, with the lowest bias and the highest percentage of accuracy (78.89%).

To the best of our knowledge, this is the first study to quantify the deviation of each DBH polygon generated by the convex hull method from the actual circular shape to examine the correlation between circularity and stem volume residuals. Although no correlation was found between convex hull circularity and stem volume residues, this study demonstrated that circularity is a robust and automatic method that can be applied preliminarily to identify non-circular 2D shapes at large scales.

Author Contributions: Conceptualization, D.P.; methodology, D.P. and A.A.; software, D.P. and A.A.; validation, D.P. and A.A.; formal analysis, D.P. and A.A.; data curation, D.P. and A.A.; writing—original draft preparation, D.P.; writing—review and editing, D.P. and A.A.; visualization, D.P. and A.A.; supervision, D.P. and A.A. All authors have read and agreed to the published version of the manuscript.

Funding: This study was financially supported by EVA4.0 “Advanced Research Supporting the Forestry and Wood-Processing Sector’s Adaptation to Global Change and the 4th Industrial Evolution” (Project No. CZ.02.1.01/0.0/0.0/16_019/0000803) of the Faculty of Forestry and Wood Sciences (FFWS) at the Czech University of Life Sciences (CULS) in Prague.

Institutional Review Board Statement: Not applicable.

Informed Consent Statement: Not applicable.

Data Availability Statement: Restrictions apply to the availability of these data. Data were obtained from (Department of Forest Management; Faculty of Forestry and Wood Sciences of the Czech University of Life Sciences Prague) and are available (from the authors) with the permission of (Czech University of Life Sciences Prague).

Acknowledgments: We would like to thank the Faculty of Forestry and Wood Sciences (FFWS).

Conflicts of Interest: The authors declare no conflict of interest.

References

- Kankare, V.; Vauhkonen, J.; Tanhuanpää, T.; Holopainen, M.; Vastaranta, M.; Joensuu, M.; Krooks, A.; Hyyppä, J.; Hyyppä, H.; Alho, P.; et al. Accuracy in estimation of timber assortments and stem distribution—A comparison of airborne and terrestrial laser scanning techniques. *ISPRS J. Photogramm. Remote Sens.* **2014**, *97*, 89–97. [[CrossRef](#)]
- Pretzsch, H.; Bielak, K.; Block, J.; Bruchwald, A.; Dieler, J.; Ehrhart, H.P.; Kohnle, U.; Nagel, J.; Spellmann, H.; Zasada, M.; et al. Productivity of mixed versus pure stands of oak (*Quercus pretraea* (Matt.) Liebl. and *Quercus robur* L.) and European beech (*Fagus sylvatica* L.) along an ecological gradient. *Eur. J. For. Res.* **2013**, *132*, 263–280. [[CrossRef](#)]
- Wang, Y.; Lehtomäki, M.; Liang, X.; Pyörälä, J.; Kukko, A.; Jaakkola, A.; Liu, J.; Feng, Z.; Chen, R.; Hyyppä, J. Is field-measured tree height as reliable as believed—A comparison study of tree height estimates from field measurement, airborne laser scanning and terrestrial laser scanning in a boreal forest. *ISPRS J. Photogramm. Remote Sens.* **2019**, *147*, 132–145. [[CrossRef](#)]
- Wang, Y.; Pyörälä, J.; Liang, X.; Lehtomäki, M.; Kukko, A.; Yu, X.; Kaartinen, H.; Hyyppä, J. In situ biomass estimation at tree and plot levels: What did data record and what did algorithms derive from terrestrial and aerial point clouds in boreal forest. *Remote Sens. Environ.* **2019**, *232*, 111309. [[CrossRef](#)]
- Forsman, M.; Börnin, N.; Holmgren, J. Estimation of tree stem attributes using terrestrial photogrammetry with a camera rig. *Forests* **2016**, *7*, 61. [[CrossRef](#)]
- Stereńczak, K.; Mielcarek, M.; Wertz, B.; Bronisz, K.; Zajaczkowski, G.; Jagodziński, A.M.; Ochał, W.; Skorupski, M. Factors influencing the accuracy of ground-based tree height measurements for major European tree species. *J. Environ. Manag.* **2019**, *231*, 1284–1292. [[CrossRef](#)]
- Panagiotidis, D.; Abdollahnejad, A.; Slavík, M. Assessment of Stem Volume on Plots Using Terrestrial Laser Scanner: A Precision Forestry Application. *Sensors* **2021**, *21*, 301. [[CrossRef](#)]
- Vaunkonen, J.; Packalen, T. Uncertainties related to climate change and forest management with implications on climate regulation in Finland. *Ecosyst. Serv.* **2018**, *33*, 213–224. [[CrossRef](#)]
- Schneider, R.; Franceschini, T.; Fortin, M.; Saucier, J.P. Climate-induced changes in the stem form of 5 North American tree species. *For. Ecol. Manag.* **2018**, *427*, 446–455. [[CrossRef](#)]
- Panagiotidis, D.; Surový, P.; Kuželka, K. Accuracy of Structure from Motion models in comparison with terrestrial laser scanner for the analysis of DBH and height influence on error behaviour. *J. For. Sci.* **2016**, *62*, 357–365. [[CrossRef](#)]

11. Panagiotidis, D.; Abdollahnejad, A.; Surový, P.; Chiteculo, V. Determining tree height and crown diameter from high-resolution UAV imagery. *Int. J. Remote Sens.* **2017**, *38*, 2392–2410. [CrossRef]
12. Yrttimaa, T.; Luoma, V.; Saarinen, N.; Kankare, V.; Junntila, S.; Holopainen, M.; Hyyppä, J.; Vastaranta, M. Structural Changes in Boreal Forests Can Be Quantified Using Terrestrial Laser Scanning. *Remote Sens.* **2020**, *12*, 2672. [CrossRef]
13. Abdollahnejad, A.; Panagiotidis, D.; Surový, P. Estimation and Extrapolation of Tree Parameters Using Spectral Correlation between UAV and Pléiades Data. *Forests* **2018**, *9*, 85. [CrossRef]
14. Lizuka, K.; Hayakawa, Y.S.; Ogura, T.; Nakata, Y.; Kosugi, Y.; Yonehara, T. Integration of Multi-Sensor Data to Estimate Plot-Level Stem Volume Using Machine Learning Algorithms—Case Study of Evergreen Conifer Planted Forests in Japan. *Remote Sens.* **2020**, *12*, 1649.
15. Pratt, V. Direct least-squares fitting of algebraic surfaces. *Comput. Graph.* **1987**, *21*, 145–152. [CrossRef]
16. Kasa, I. A circle fitting procedure and its error analysis. *IEEE Trans. Instrum. Meas.* **1976**, *IM-25*, 8–14. [CrossRef]
17. Taubin, G. Estimation of planar curves, surfaces, and non-planar space curves defined by implicit equations with applications to edge and range image segmentation. *IEEE Trans. Pattern Anal. Mach. Intell.* **1991**, *13*, 1115–1138. [CrossRef]
18. Chernov, N. *Circular and Linear Regression: Fitting Circles and Lines by Least Squares*; Taylor & Francis: Boca Raton, FL, USA, 2011; ISBN 9781439835906.
19. Fitzgibbon, A.; Pilu, M.; Fisher, R.B. Direct least square fitting of ellipses. *IEEE Trans. Pattern Anal. Mach. Intell.* **1999**, *21*, 476–480. [CrossRef]
20. Fischler, M.A.; Bolles, R.C. Random sample consensus—A paradigm for model-fitting with applications to image-analysis and automated cartography. *Commun. ACM* **1981**, *24*, 381–395. [CrossRef]
21. Schnabel, R.; Wahl, R.; Klein, R. Efficient RANSAC for Point-Cloud Shape Detection. *Comput. Graph. Forum* **2007**, *26*, 214–226. [CrossRef]
22. Olofsson, K.; Holmgren, J.; Olsson, H. Tree Stem and Height Measurements using Terrestrial Laser Scanning and the RANSAC Algorithm. *Remote Sens.* **2014**, *6*, 4323–4344. [CrossRef]
23. Panagiotidis, D.; Abdollahnejad, A.; Surový, P.; Kuželka, K. Detection of Fallen Logs from High-Resolution UAV Images. *N. Z. J. For.* **2019**, *49*. [CrossRef]
24. Fan, G.; Nan, L.; Chen, F.; Dong, Y.; Wang, Z.; Li, H.; Chen, D. A New Quantitative Approach to Tree Attributes Estimation Based on LiDAR Point Clouds. *Remote Sens.* **2020**, *12*, 1779. [CrossRef]
25. Mikita, T.; Janata, P.; Surový, P. Forest Stand Inventory Based on Combined Aerial and Terrestrial Close-Range Photogrammetry. *Forests* **2016**, *7*, 165. [CrossRef]
26. Astrup, R.; Ducey, M.J.; Granhus, A.; Ritter, T.; Von Lüpke, N. Approaches for estimating stand-level volume using terrestrial laser scanning in a single-scan mode. *Can. J. For. Res.* **2014**, *44*, 666–676. [CrossRef]
27. Mayamanikandan, T.; Reddy, R.S.; Jha, C. Non-Destructive Tree Volume Estimation using Terrestrial Lidar Data in Teak Dominated Central Indian Forests. In Proceedings of the 2019 IEEE Recent Advances in Geoscience and Remote Sensing: Technologies, Standards and Applications (TENGEARSS), Kochi, India, 17–20 October 2019; pp. 100–103.
28. Haglöf Sweden Laser Geo. Available online: <https://haglofsweden.com/project/laser-geo-2> (accessed on 22 October 2003).
29. Haglöf Sweden DP II Computer Caliper. Available online: <https://haglofsweden.com/project/dp-ii-computer-caliper> (accessed on 22 October 2003).
30. Trimble Realworks 10.2 User Guide. 2017. Available online: <https://www.trimble.com/3d-laser-scanning/realworks.aspx> (accessed on 12 October 2019).
31. Zhang, W.; Qi, J.; Wan, P.; Wang, H.; Xie, D.; Wang, X.; Yan, G. An Easy-to-Use Airborne LiDAR Data Filtering Method Based on Cloth Simulation. *Remote Sens.* **2016**, *8*, 501. [CrossRef]
32. Girardeau-Montaut, D. CloudCompare. 2017. Available online: <http://www.danielgm.org> (accessed on 19 December 2016).
33. ESRI ArcGIS Pro 2.4.2. Available online: <https://www.esri.com/en-us/arcgis/products/arcgis-pro/resources> (accessed on 21 May 2020).
34. Corral-Rivas, J.J.; Barrio-Anta, M.; Aguirre-Calderón, O.A.; Diéguez-Aranda, U. Use of stump diameter to estimate diameter at breast height and tree volume for major pine species in El Salto, Durango (Mexico). *Forestry* **2007**, *80*, 29–40. [CrossRef]
35. St-Onge, B.; Achaichia, N. Measuring forest canopy height using a combination of LIDAR and aerial photography data. *Int. Arch. Photogramm. Remote Sens. Spat. Inf. Sci.* **2001**, *34*, 22–24.
36. About ArcGIS. Mapping & Analytics Software and Services. Available online: <https://www.esri.com/en-us/arcgis/aboutarcgis/overview> (accessed on 22 February 2021).
37. Rousseeuw, P.J.; Kaufman, L. Finding groups in data. *Ser. Probab. Math. Stat.* **2003**, *34*, 111–112.
38. Bucher, I. CircleFit. 2004. Available online: <https://se.mathworks.com/matlabcentral/fileexchange/5557-circle-fit/content/circfit.m> (accessed on 15 December 2016).
39. Petráš, R.; Pajtík, J. Sústava česko-slovenských objemových tabuliek drevín. *Lesn. Čas.* **1991**, *37*, 49–56.
40. Kořen, M.; Mokroš, M.; Bucha, T. Accuracy of tree diameter estimation from terrestrial laser scanning by circle-fitting methods. *Int. J. Appl. Earth Obs. Geoinf.* **2017**, *63*, 122–128. [CrossRef]
41. Saarinen, N.; Kankare, V.; Vastaranta, M.; Luoma, V.; Pyoral, J.; Tanhuanpaa, T.; Liang, X.L.; Kaartinen, H.; Kukko, A.; Jaakkola, A.; et al. Feasibility of Terrestrial laser scanning for collecting stem volume information from single trees. *ISPRS J. Photogramm. Remote Sens.* **2017**, *123*, 140–158. [CrossRef]

-
42. Pitkänen, T.P.; Raunonen, P.; Liang, X.; Lehtomäki, M.; Kangas, A. Improving TLS-based stem volume estimates by field measurements. *Comput. Electron. Agric.* **2021**, *80*, 105882. [[CrossRef](#)]
 43. Fassnacht, F.E.; Hartig, F.; Latifi, H.; Berger, C.; Hernández, J.; Corvalán, P.; Koch, B. Importance of sample size, data type and prediction method for remote sensing-based estimations of aboveground forest biomass. *Remote Sens. Environ.* **2014**, *154*, 102–114. [[CrossRef](#)]
 44. Shin, J.; Temesgen, H.; Strunk, J.L.; Hilker, T. Comparing Modeling Methods for Predicting Forest Attributes Using LiDAR Metrics and Ground Measurements. *Can. J. Remote Sens.* **2016**, *42*, 739–765. [[CrossRef](#)]